An insight into using DFT data for Calphad modeling of solid phases in the third generation of Calphad databases, a case study for Al

Sedigheh Bigdeli[1], Li-Fang Zhu[2], Albert Glensk[2], Blazej Grabowski[2], Bonnie Lindahl[3], Tilmann Hickel[2] and Malin Selleby[1]

[1]Materials Science and Engineering, KTH Royal Institute of Technology, SE-100 44 Stockholm, Sweden
e-mail: sedigheh@kth.se
[2]Max-Planck-Institut für Eisenforschung GmbH, Max-Planck-Straße 1, Düsseldorf 40237, Germany
[3]Swerea KIMAB AB, P.O. Box 7047, SE-164 07 Kista, Stockholm, Sweden

Abstract In developing the next generation of Calphad databases, new models are used in which each term contributing to the Gibbs energy has a physical meaning. To continue the development, finite temperature density-functional-theory (DFT) results are used in the present work to discuss and suggest the most applicable and physically based model for Calphad assessments of solid phases above the melting point (the breakpoint for modeling the solid phase in previous assessments). These results are applied to investigate the properties of a solid in the superheated temperature region and to replace the melting temperature as the breakpoint with a more physically based temperature, i.e., where the superheated solid collapses into the liquid. The advantages and limitations of such an approach are presented in terms of a new assessment for unary aluminum.

Keywords: Al, Calphad modeling, *ab initio*, density-functional-theory.

1 Introduction

New models have been suggested and used during recent years [1-7] for re-modeling thermodynamic properties of pure elements (unaries). The goal is to develop the next generation of Calphad databases, i.e., databases that are valid down to 0 K and have a more physical meaning compared to the earlier descriptions. For example, the approach suggested in Ref. [1] for modeling thermodynamic properties of pure Fe was already successfully applied to unaries, e.g., Cr, Ni [2] Mn [3], metastable phases of Mn and Fe [4], pure Co [5] and [6], and Pb [7]. In this approach, the Einstein model is used for modeling harmonic vibrations of atoms. Anharmonic vibrations and electronic contributions are taken into account by polynomials fitted to experimental data. Although these models are still governed by efficiency, they provide a first step towards a more physical description over the previous phenomenological models [8], and they have been shown [2-7] to describe thermodynamic properties from 0 K to above the melting point in good agreement with experimental data.

The special properties of Al, such as its light weight, low melting point (934 K), high strength-to-weight ratio and corrosion resistance of its alloys, have made this metal a key element for many different applications. Al is expected to have simple thermophysical properties, since it is non-magnetic and in the solid state only observed in the fcc crystal structure. It therefore belongs to one of the best studied metals. The main interest, however, lies in using Al as an alloying element as well as a base element for many light-weight alloys. Therefore, an improvement of the thermodynamic description of Al is mainly done with the goal to achieve a more reliable design of multicomponent materials. In this respect, a proper description of the heat capacity C_p of the solid phase is crucial also above the melting point of Al. Polynomial basis functions used in a previous assessment of this element in Ref. [8] result however in an artificial kink in C_p at the melting point. This kink is unphysical and causes problems for higher order systems with elements with a higher melting temperature than Al [9]. Possible solutions to this problem are given in the present work employing results from atomistic first principles methods, i.e., density-functional-theory (DFT), as well as Calphad.

An extensive literature overview of experimental measurements, DFT calculations and Calphad modeling of pure Al is presented in the next section, Sec. 2. In Sec. 3 a new description of Al is presented along the lines of previous assessments within the third generation of database development [1-7]. In Sec. 4, the physical behavior of the solid phase above the melting point is discussed employing DFT-based results and calculations. Based on the insights gained from the atomistic simulations, an alternative description of this temperature regime is suggested in Sec. 5 and compared with the approach discussed in Sec. 3.

2 Literature review

There has been an enormous interest in experimentally investigating pure Al. Regarding thermodynamic properties, Refs. [10] [11] [12] [13] [14] [15] [16] [17] [18] [19]measured the heat capacity of pure Al at low temperatures, and Brooks and Bingham [20] and Dosch and Wendlandt [21] at high temperatures. Brooks and Bingham [20] derived the different contributions to the heat capacity, e.g., electronic, anharmonic and vacancy formation, with the help of experimental thermal expansion data from Refs. [22] and [23]. Leadbetter [24] investigated anharmonic and electronic effects in Al utilizing the theoretical heat capacity at constant volume. Awbery and Griffiths [25] and Speros and Woodhouse [26] measured the heat of fusion and melting temperature of pure Al by drop calorimetry and differential scanning calorimetry, respectively.

The thermal expansion of this element has also attracted attention of many researchers; Refs. [27] [28] [29] [30] [31] [32] [33] [34] [35] [36] [37] [38] [39] [40] [41] [42] [43] [44] [45] [46] [47] [48] measured the expansion of pure Al by different techniques. Further, Kamm and Alers [49] measured the change of elastic moduli of pure Al with temperature and from these results, determined the Debye temperature of Al to be 430.3 K. Gerlich and Fisher [50] calculated the Grüneisen parameter from similar measurements at high temperatures. The Grüneisen parameter was also calculated by Thomas [51] and Ho and Ruoff [52] from measurements of the sound velocity in different directions and at several temperatures in pure Al.

Since electronic contributions are small in Al compared to other metallic elements, they can be neglected when separating different contributions to the heat capacity and this makes it possible to evaluate the thermal vacancy contribution to the heat capacity by direct or indirect techniques. Feder and Nowick [53] estimated the variation of the thermal vacancy concentration in this element with temperature by measuring the thermal expansion of pure Al by X-ray diffraction and dilatometry. It was concluded that the large increase of thermal expansion near the melting point is due to anharmonicity rather than thermal vacancies. However, Refs. [54], [55], [56], [57] and [58] showed that the thermal vacancy concentration increases exponentially with temperature and although the absolute contribution is rather small, it has an effect on the shape of the heat capacity curve close to the melting point. This has been confirmed more recently by highly accurate DFT calculations [59]. Hehenkamp [60] measured the vacancy concentration of pure Al using a Debye-Scherrer technique and predicted a linear Arrhenius behavior for this contribution. The conclusion was however shown to be invalid at lower temperatures by Glensk *et al.* [61] using DFT calculations.

The fast progress in computational resources and techniques in the last two decades triggered many investigations on thermodynamic properties calculated with DFT. Al in particular has been used as a case study for different techniques due to its simple properties, e.g., having only one allotropic structure (fcc), absence of magnetism and low melting point. Refs. [62] [63] [64] [65] [66] [67] [68] [69] [70] [71] [72] [73] [74] [75] used used different techniques based on quantum theory (DFT) for calculating mechanical and thermodynamic properties of fcc and/or liquid Al. Results of these investigations have been validated by experimental measurements of the phonon dispersion using the neutron diffraction method by Refs. [76-78].

The pressure-volume phase diagram of Al was experimentally investigated by Hänström and Lazor [76], while Refs [77], [78] and [79] used *ab initio* molecular dynamics simulations to calculate this phase diagram. Boehler and Ross [80] investigated melting of Al under high pressure and reported a transition from fcc to hcp at 2 Mbar. The molar volume as a function of temperature at atmospheric pressure was assessed using the Calphad approach by Lu *et al.* [81] and Hallstedt *et al.* [82].

3 Calphad modeling

For Calphad modeling of the solid phase (fcc) below the melting temperature we have applied the approach suggested in Ref. [1]. In this approach, each term contributing to the Gibbs energy has a physical meaning according to:

$$G = E_0 + \frac{3}{2}R\theta_E + 3RT\ \ln\left[1 - \exp(-\frac{\theta_E}{T})\right] - \frac{a}{2}T^2 - \frac{b}{20}T^4 \qquad T < T_\mathrm{m}\ , \qquad (1)$$

where Θ_E is the Einstein temperature of the solid phase representing the contribution due to harmonic vibrations of the atoms and the parameters a and b represent the Sommerfeld-temperature contribution to the electronic heat capacity and a higher order correction due to anharmonicity, respectively. R is the gas constant and E_0 is the cohesive energy at 0 K. These parameters were fitted to the experimental heat capacity and enthalpy data up to the melting point, T_m.

To model the solid phase above the melting point, Ref. [1] suggests the expression:

$$G = \frac{3}{2}R\theta_E + 3RT\ \ln\left[1 - \exp(-\frac{\theta_E}{T})\right] + H' - S'T + a'T(1 - \ln T) - \frac{b'}{30}T^{-5} - \frac{c'}{132}T^{-11} \qquad T \geq T_\mathrm{m}\ , \qquad (2)$$

where additional terms are present compared to Eq. (1) that cannot be directly linked to physical mechanisms. Instead, According to Ref. [1], the parameters, a', b' and c' are calculated assuming that the heat capacity and its first derivative should have identical values at the melting point when calculated from Eqs. (1) and (2). The heat capacity of the solid calculated form Eq. (2) should give a value equal to the heat capacity of the liquid phase at an arbitrary temperature much beyond the melting point, e.g., ≈ 3000 K. H' and S' are the enthalpy and entropy of melting of the solid phase respectively. Validating these assumptions is the main purpose of this article, for which the ab initio calculations were used to investigate the behavior of superheated solid at high temperatures. The results for the solid phase presented below in the present section are based on Eq. (2). In Sec. 5 alternative descriptions will be investigated.

The experimental data recommended by Desai [83] were used for optimization in the present work. The resulting Gibbs energy descriptions for both phases are presented in Table 1. The liquid phase was not assessed in the present work, since we mainly focused on modeling the solid phase at high temperatures.

Table 1 Summary of the Gibbs energy expressions for Al at 1 bar (10^5 Pa).

FCC	$-8205 - 2.225\times10^{-3}T^2 - 3.706\times10^{-8}T^3 - 2.846\times10^{-13}T^5 + G_{EIN}(287)$	$0.0<T<934$
	$-13613 + 65.574T - 9.0754\ .\ T\ln(T) - 6.335\times10^{16}T^{-5} + 1.087\times10^{34}T^{-11} + G_{EIN}(287)$	$934<T<6000$
Functions	$G_{EIN}(\theta) = 1.5R\theta + 3RT\ln(1 - \exp(\theta/T))$	

Figure 1 shows the heat capacity calculated from the description in Table 1, compared with the experimental data and previous assessment from SGTE [8] (red dashed curve). The results from the present work show a good agreement with the experimental data used for the optimization (Desai [86]) and also change smoothly at the melting point in contrast to the SGTE description [8] where an artificial kink is observed at the melting temperature. Below 100 K (inset picture in the lower left corner), the agreement between the present work and the experimental data is better than for SGTE but still not perfect, due to the limitations of the Einstein model. Since no significant phase transformation occurs in this region and since our focus here is on high temperatures, a further optimization beyond the suggestions in Ref. [1] was not performed. It should be mentioned that the

SGTE function is not valid at a temperature below 298.15 K and the red curve in this figure was extrapolated outside its validity range just for comparison.

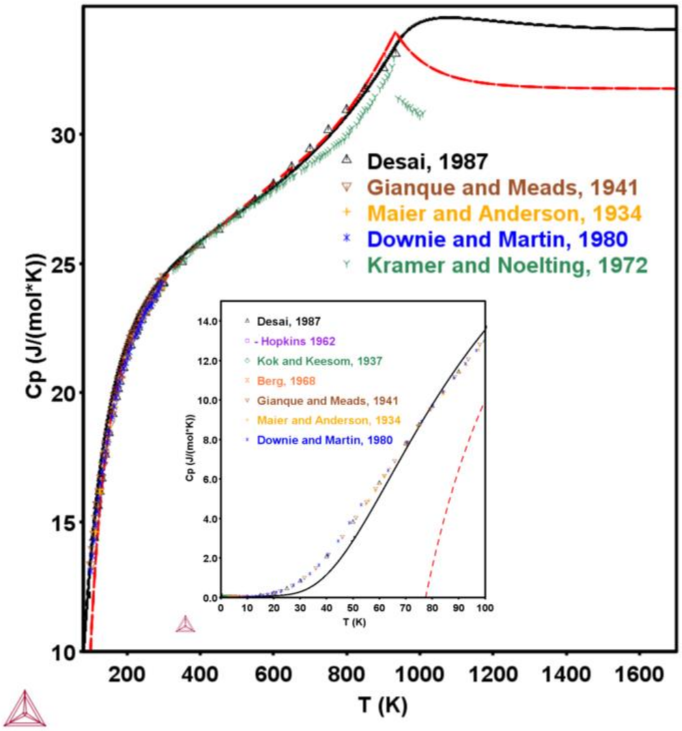

Fig. 1. Heat capacity of fcc Al, calculated from the description given in Table 1 (black curve) compared to experimental data and SGTE [8] (red dashed curve).

4 *Ab initio* calculations up to and beyond the melting point

We have shown in the previous section that, if the method suggested in Ref. [1] is used for modeling the solid phase, a good agreement with experimental data can be obtained and the model is physically more sound for low temperatures as compared to the SGTE description [8]. In addition, the artificial kink in the heat capacity curve from SGTE for the solid at the melting point (Fig. 1) can be avoided.

However, modeling the solid phase above the melting point according to Eq. (2) is not underpinned by physical consideration and therefore does not necessarily reflect reality. In principle, an (overheated) solid phase can also be metastable in this temperature regime, while the stability of the liquid phase is mainly due to its entropy. Thus, we have attempted to use DFT results as the basis for the Calphad modeling of the solid phase above the melting point, since this allows a description of the correct physics while suppressing the occurrence of the liquid state.

Thermodynamic properties of pure Al were previously calculated in Refs. [59] and [61] using highly accurate DFT-based methods, including all relevant excitations up to the melting point. In Ref. [59], the UP-TILD (*upsampled thermodynamic integration using Langevin dynamics*) method was introduced and applied to calculate anharmonic contributions to the Gibbs energy for fcc-Al from 0 K up to the (experimental) melting temperature. This methodology was subsequently used in Ref. [61] to investigate the contribution of the vacancies in Al and Cu in more detail. In the present work, the heat capacity data from Grabowski *et al.* [59] in combination with the vacancy data from Ref. [61] (using in particular the GGA-PBE data) have been utilized for the Calphad modeling in Sec. 5. To be able to investigate the behavior of the solid phase beyond the experimental melting point, the different contributions, i.e., quasiharmonic, electronic, anharmonic and vacancies have been extrapolated into this high temperature region, as described in the following.

The quasiharmonic Helmholtz free energy was extrapolated analytically to temperatures above the melting point by employing the analytical dependencies derived for $T<T_m$ [59]. The volume dependence of the quasiharmonic free energy was interpolated using a second order polynomial. The calculated electronic free energy points were parameterized using a linear and quadratic dependence in temperature and volume, respectively. The parameterization of the anharmonic contribution was based on renormalized frequencies ω_{ah} as described in Ref. [59]. The same procedure was used to obtain the anharmonic free energy surface above the melting point. To extrapolate the vacancy contribution, we have utilized the Gibbs energy of formation as computed previously in Ref. [61] containing all relevant excitation mechanisms. Since the inclusion of anharmonic vibrations leads to a breakdown of the Arrhenius prediction, i.e., to a strongly non-linear temperature dependence of the Gibbs energy of formation [61], it was necessary to employ a non-linear third-order polynomial to fit the data at $T<T_m$. This fit was then used for the extrapolation of the Gibbs energy of formation, from which the vacancy concentration and thus the vacancy contribution to the total bulk Gibbs energy could be calculated.

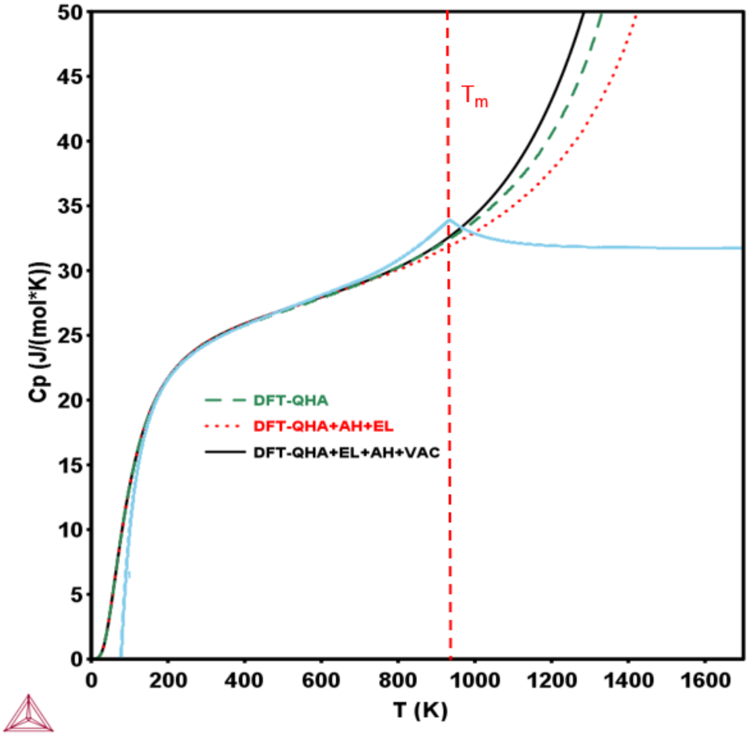

Fig. 2. Heat capacity of fcc-Al based on DFT results from Refs. [59] and [59]. For T>934 K the low temperature data (T<934 K) have been extrapolated including different contributions (QHA=quasiharmonic, AH=anharmonic, EL=electronic, VAC=vacancies; see text for more details). The light blue line shows SGTE data [8].

The extrapolated DFT results shown in Fig. 2 reveal that the heat capacity of the solid increases moderately with temperature until the melting point, followed by a drastic increase above the melting point. The equilibrium volume shows a similar behavior (Fig. 3), suggesting that the solid "explodes" at high temperatures. The sharp increase in the volume and heat capacity goes along with a sharp decrease of the Gibbs energy of the solid, leading to a re-stabilization of the fcc phase above the melting point if these extrapolations are used as input to a Calphad assessment. However, one should be careful in interpreting these data above the melting temperature. At a certain temperature, the superheated solid will become unstable and inevitably collapse to the liquid phase. The reason why this is not observed in the DFT data is the fact that these data have been extrapolated from the stable regime and thus, they do not contain the notion of an instability.

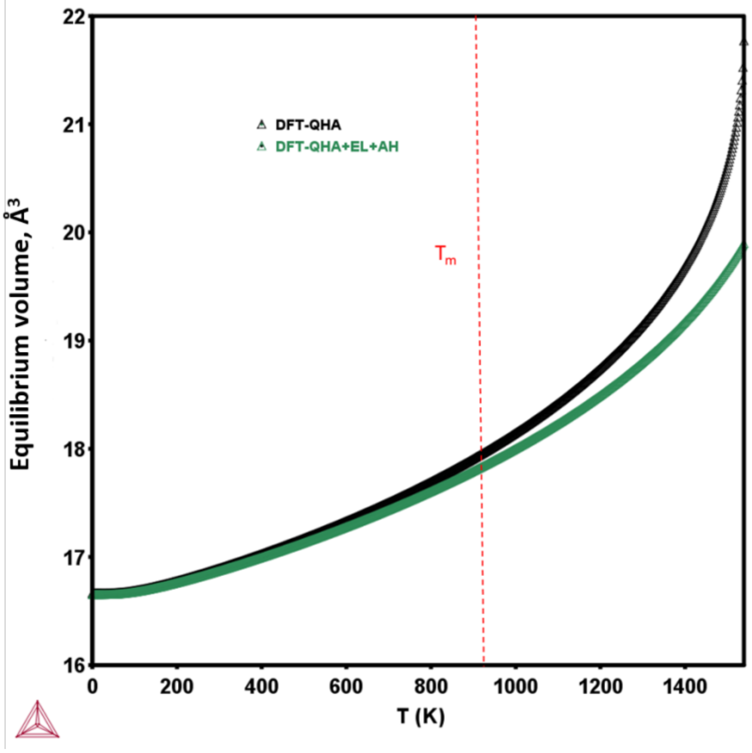

Fig. 3. Equilibrium volume of fcc-Al, data for T<934 K are from Ref. [59]. For T>934, the low temperature data (T<934 K) have been extrapolated (see text).

Explicit simulations of the superheated solid are required to have a better understanding of when the unavoidable transition to the liquid phase occurs. Using direct DFT simulations for that purpose is not practical due to the finite time and length scale restrictions. We have therefore employed a DFT-optimized embedded atom method (EAM) potential, fitted to a wide-range of DFT (GGA-PBE) molecular dynamics simulations of solid Al (fitting was performed with the MEAMfit code [84]) to simulate the superheated conditions. The approach taken is in the spirit of the TU-TILD (*two-stage upsampled thermodynamic integration using Langevin dynamics*) method as introduced in Ref. [85] where such optimized potentials were shown to be a highly efficient reference for free energy calculations of the solid phase. More recent work has shown that the TU-TILD method is also applicable to the liquid phase [86].

The obtained results show that the superheated solid collapses to the liquid at 1039 K. We will call that temperature, where the solid becomes intrinsically unstable T_{inst}, following Ref. [9]. T_{inst} is determined by the transition point from solid to liquid during the superheating simulation. However, we cannot directly transfer the absolute T_{inst} temperature to experiment because of a general underestimation of the experimental melting temperature. The melting point calculated from our fitted EAM potential, determined by the interface method [87], is $T_m^{pot} = 819$ K, which is lower than the experimentally measured one, $T_m^{exp} = 933$ K. This difference is only partially due to a discrepancy in the EAM potential itself. Another source of error comes from the exchange-correlation functional employed in the DFT simulations (GGA-PBE). Our previous work [94] showed that melting temperatures obtained with GGA-PBE underestimate the melting point, while the LDA functional tends to overestimate the melting point. For the present case, additional calculations with an EAM fitted to LDA energies confirm a higher melting point than with the GGA-PBE EAM.

In order to determine an experimental T_{inst} we have to properly take into account the lower melting temperature of the EAM potential. One possibility would be to shift the computed $T_{inst}^{pot} = 1039$ K by the difference $T_m^{exp} - T_m^{pot} = 114$ K giving $T_{inst}^{exp} \sim 1150$ K. Another option is to rescale $T_{inst}^{pot} = 1039$ K by the ratio of $\frac{T_m^{exp}}{T_m^{pot}} = 1.14$ giving $T_{inst}^{exp} \sim 1200$ K. It cannot be said whether one of these choices would reflect better the experimental T_{inst}. In any case we should expect an additional impact on the instability temperature due to the interatomic potential and due to the exchange-correlation functional. However, for our purposes an estimate of experimental T_{inst} is sufficient and we have decided to utilize $T_{inst}^{exp} \sim 1200$ K in the following.

Thus, the extrapolated DFT data shown in Fig. 2 should be used only up to a temperature of about 1200 K in the Calphad modeling. The remaining question is how to model thermodynamic properties above this temperature. This will be discussed in the following section.

It is worth mentioning that during the superheating simulations, the supercell size and vacancy effects on T_{inst} of Al were tested. The supercell sizes of 8×8×8, 10×10×10, 12×12×12, 14×14×14 and 16×16×16 (in terms of the cubic fcc cell) were used and it was found that there is only a small variation of T_{inst} in the range of 20 K. As for the vacancy effect, a typical vacancy concentration of ~0.001 at the melting point, was simulated and only a small effect on T_{inst} (~10 K) was found. We increased the vacancy concentration further to 0.003 and still found a negligible impact on T_{inst}.

We note also that a comparison of our computed T_{inst} temperature with experimental measurements should be done with care. Our calculations correspond to a homogenous melting which is hardly accessible in experiments. In general, measurements of a superheated solid are very difficult and have been mostly attempted for lower melting elements than Al (in fact, often using Al as a matrix) [88] The two available experiments for Al superheating show a large scatter: oxide-coated Al particles reveal a small pressure-induced overheating to about 960 K [88], while femtosecond electron diffraction can drive the bulk system to a highly unstable state at 1400 K [89]. The reason or the immense scatter in the overheating temperature is that the amount of overheating depends strongly on the experimental conditions and which mechanisms are available to initiate the melting process. The strong impact of boundary conditions (e.g., geometry of the nanoparticles) on the overheating temperature was also shown in a recent phase field modeling study [90].

5 Coupling DFT and Calphad for modeling the solid phase

As mentioned in the beginning of the previous section, our goal is to use the DFT results as an input in the Calphad modeling to increase the physical content of the solid's behavior above the melting point. To do that, firstly, the breakpoint for Eqs. (1) and (2) should change from T_{m} to T_{inst}, i.e., 1200 K (the transition of the superheated solid to the liquid). Secondly, the heat capacity data from the extrapolated DFT results or enthalpy data calculated by the method suggested in the previous section should be used to fit the Gibbs energy in the temperature range T_{m} to T_{inst}.

It is, however, not enough to limit the description of the solid phase to temperatures below 1200 K, since the Calphad method is based on the Gibbs energy minimization for finding the stable state under equilibrium conditions and each phase needs to have a description for making energy minimization possible [96]. Ideally the description of pure, solid Al above T_{inst} does not enter any result, since it does not describe proper physics. However, it should be done such that further corrections of artificial effects are avoided. This is particularly important in higher-order systems, i.e., Al-alloys with elements that have a melting point higher than T_{inst} of Al.

It therefore remains necessary to model the solid phase above T_{inst}. If the heat capacity of the solid is forced to reach the heat capacity value for liquid at very high temperatures, e.g., 3000 K, as was done for the Calphad modeling in Sec. 3, a very strong curvature appears at 1200 K, as shown in Fig. 4 (black solid line). This treatment clearly does not improve the SGTE description [6] but worsens the kink problem in the solid phase at the melting point for this description (red dashed curve in Fig. 1). Thus, such a treatment cannot be used. One way to avoid such a problem is to keep the heat capacity of the solid constant at 1200 K and not to force it back to the heat capacity of the liquid.

Results for the heat capacity based on this treatment are shown in Fig. 5 in (curve I), compared to the model suggested in Sec. 3 (curve II) and SGTE [8] description (curve III).

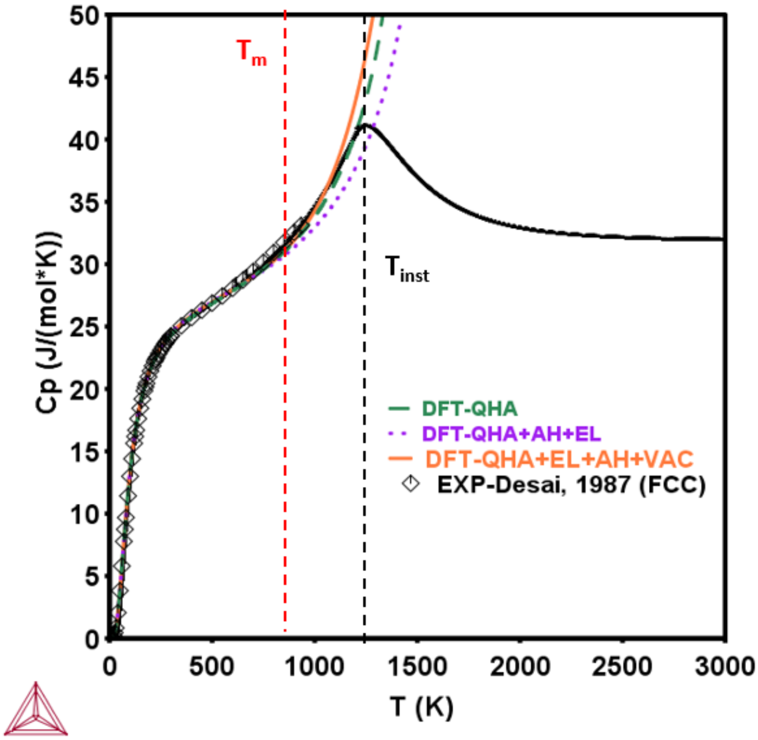

Fig. 4. Heat capacity of fcc pure Al, optimized based on the experimental results from [59], compared with experimental results from Desai [83]. The sharp kink in the fcc description makes this treatment inappropriate for improving SGTE description [8] and thus, cannot be used.

The modeling up to 1200 K by Eq. (1) corresponds to a perfect superheated solid, i.e., without an explicit vacancy term. This contribution is negligible at low temperatures, but above ~600 K up to the melting point, it is significant, Ref. [56] and [57-59]. Therefore, the thermal vacancy contribution, calculated by *ab initio* [61], has been subtracted from the experimental data. In this way it is avoided that they indirectly enter the parameterization. This is the reason for the small difference between the experimental [83] and DFT [59] heat capacity when reaching the melting temperature in Fig. 5.

Thermal vacancies should be treated separately as a structure-dependent contribution in Calphad modeling, but a general approach that works for all materials systems equally well is still pending. We note that other practical relationships, for example those suggested in Refs. [61] and [91] can be used to treat the thermodynamic contribution of vacancies.

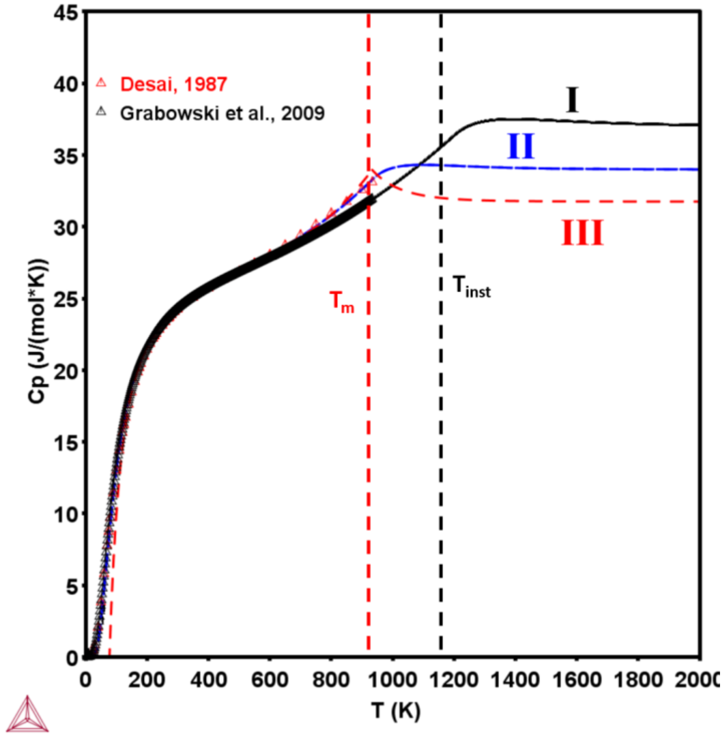

Fig. 5. Heat capacity of different phases of pure Al: I) fcc phase modelled based on DFT data for the superheated solid, II) fcc phase based on the model of Ref. [1] and III) SGTE description [8]. Experimental data in red, from Desai [83], and C_p data from DFT [61] in black symbols.

The thermodynamic description for the fcc phase (curve I in Fig. 5), which is based on the DFT results, is presented in Table 2.

Table 2 Summary of the Gibbs energy expressions for Al at 1 bar (10^5 Pa), based on DFT data for fcc phase.

FCC	$-8135-1.232\times10^{-3}T^2-8.337\times10^{-7}T^3-3.315\times10^{-14}T^5+G_{EIN}(281)$	$0.0<T<1200$
	$-17360++90.54T-12.07T\ln(T)-2.742\times10^{17}T^{-5}+2.217\times10^{35}T^{-11}+G_{EIN}(281)$	$1200<T<6000$
Functions	$G_{EIN}(\theta)=1.5R\theta+3RT\ln(1-\exp(\theta/T))$	

6 Conclusion

Within the present work we have proposed a new model for the thermodynamic properties of pure Al, based on physically more sound assumptions than used in the original SGTE assessment [6]. The description of the solid phase below the melting point follows previously suggested methods [1]. We have here specifically tested the application of these methods beyond the melting point T_m up to an instability temperature T_{inst} of 1200 K.

The extension has been done in three steps: First, DFT-based MD simulations have been utilized, to achieve an accurate, precise and consistent description of the heat capacity below the melting temperature, where these calculations are numerically feasible. Second, the analytical dependencies achieved in this approach have been extrapolated to 1200 K. Third, the resulting curve has been used to fit the Calphad model parameters [1] such that a description up to 1200 K was achieved.

The temperature T_{inst} itself has been determined from MD simulations with an EAM potential that has been parameterized by DFT calculations. In the case of Al, it turns out that the instability temperature is only 250 K above the melting temperature and connected with a strong increase of the heat capacity. This makes the transition to a parameterization of the solid phase above T_{inst} challenging. In particular, the vacancy contribution tends to diverge very quickly and therefore needs to be treated separately. A systematic evaluation of the approach presented here requires the consideration of multicomponent alloys, in which solid phases exist above the melting temperature of Al. Despite the challenges in the case of Al, the new approach must be applied to other elements in order to evaluate its usefulness.

Acknowledgments

The work was performed within the VINN Excellence Center Hero-m, financed by VINNOVA (Grant number 2012-02892), the Swedish Governmental Agency for Innovation Systems, Swedish industry, and KTH Royal Institute of Technology. Funding by the European Research Council (ERC) under the EU's Horizon 2020 Research and Innovation Programme (Grant No. 639211) is gratefully acknowledged. The authors gratefully acknowledge Drs. Qing Chen, Huahai Mao, Ursula Kattner, Alexandra Khvan, Bengt Hallstedt, Profs. Alan Dinsdale, Andrei Ruban, John Ågren, Bo Sundman and Jörg Neugebauer for valuable discussions.

Bibliography

[1] Q. Chen and B. Sundman, «Modeling of thermodynamic properties for Bcc, Fcc, liquid, and amorphous iron,» *Journal of Phase Equilibria,* vol. 22, n. 6, pp. 631-644, 2001.

[2] W. Xiong and M. Selleby, *unpublished,* 2014.

[3] S. Bigdeli, H. Mao and M. Selleby, «On the third-generation Calphad databases: An updated description of Mn,» *Physica Status Solidi (B),* vol. 252, p. 2199, 2015.

[4] S. Bigdeli, H. Ehteshami, Q. Chen, H. Mao, P. Korshavy and M.Selleby, «New description of metastable hcp phase for unaries Fe and Mn: Coupling between first-principles calculations and CALPHAD modeling,» *Phys. Status Solidi B,* vol. 1836, n. 9, pp. 1830-1836, 2016.

[5] Z. Li, S. Bigdeli, H. Mao, Q. Chen and M. Selleby, «Thermodynamic evaluation of pure cobalt for the third generation of thermodynamic databases,» *Phys. Status Solidi B,* vol. 254, n. 2, February 2017 , pp. 1-11, 2017.

[6] Li, Z., Mao, H. and Selleby, M., «Thermodynamic Modeling of Pure Co Accounting Two Magnetic States for the Fcc Phase,» *Journal of Phase Equilibia and Diffusion,* pp. DOI: 10.1007/s11669-018-0656-x, 2018.

[7] Khvan, A. and Dinsdale, A. and Uspenskaya, I. and Zhilin, M. and Babkina, T and Phiri, A., «A thermodynamic description of data for pure Pb from 0 K using the

expanded Einstein model for the solid and the two state model for the liquid phase,» *Calphad ,* vol. 60, pp. 144-155, 2018.

[8] A. Dinsdale, «SGTE data of pure elements,» *Calphad,* vol. 15, n. 4, pp. 317-425, 1991.

[9] M. Palumbo, B. Burton, A. Costa e Silva, B. Fultz, B. Grabowski, G. Grimvall, B. Hallstedt, O. Hellmann, B. Lindahl, P. Turchi, and W. Xiong, «Thermodynamic modelling of crystalline unary phases,» *Physica Status Solidi (B) Basic Research,* vol. 251, n. 1, pp. 14-32, 2014.

[10] E. Eastman, «The specific heats of magnesium, calcium, zinc, aluminum and silver at high temperatures,» *American Chemical Society Legacy Archives,* vol. 46, pp. 1178-1183, 1924.

[11] J. A. Kok and w. H. Keesom, «Measurements of the atomic heat of aluminium from 1.1 to 20° K,» *Physica,* vol. 4, n. 9, pp. 835-842, 1937.

[12] W. F. Giauque and P. F. Meads, «The Heat Capacities and Entropies of Aluminum and Copper from 15 to 300° K,» *Journal of the American Chemical Society,* vol. 63, pp. 1897-1901, 1941.

[13] T. E. Pochapsky, «Heat capacity and resistance measurements for aluminum and lead wires,» *Acta Metallurgica,* vol. 1, p. 747, 1953.

[14] K. I. Hirano, H. Maniwa and Y. Takagi, «Specific Heat Measurements on Quench Annealed Al, Cu and alpha-phase alloys of Cu,» *J. Phys. Soc. Japan,* vol. 10, p. 909, 1955.

[15] B. Goodman, «Chaleur - La chaleur spécifique des supraconducteurs Al, Sn et V au-dessous de 1 K,» *Comptes Rendus Hebdomadaires des Seances de l Academie des Sciences,* vol. 12, p. 2899, 1957.

[16] N. E. Phillips, «Heat capacity of aluminum between 0.1 K and 4.0 K,» *Physical Review,* vol. 114, n. 1954, p. 676, 1959.

[17] M. Dixon, F. E. Hoare, T. M. Holden and D. E. Moody, «The Low Temperature Specific Heats of Some Pure Metals (Cu, Ag, Pt, Al, Ni Fe Co),» *Proceedings of the Royal Society A: Mathematical, Physical and Engineering Sciences,* vol. 285, n. 1403, p. 561, 1965.

[18] W. T. Berg, «Heat capacity of Aluminum between 2.7 and 20 K,» *Physical Review,* vol. 167, n. 3, pp. 583-586, 1968.

[19] D. B. Downie and J. F. Martin, «An adiabatic calorimeter for heat-capacity measurements between 6 and 300 K. The molar heat capacity of aluminium,» *The Journal of Chemical Thermodynamics,* vol. 12, p. 779, 1980.

[20] C. R. Brooks and R. E. Bingham, «The specific heat of aluminum from 330 to 890 K and contributions from the formation of vacancies and anharmonic effects,» *Journal of Physics and Chemistry of Solids,* vol. 29, pp. 1553-1560, 1968.

[21] E. L. Dosch and W. W. Wendlandt, «The deltatherm dynamic adiabatic calorimeter: some applications,» *Thermochimica Acta,* vol. 1, n. 2, pp. 181-189, 1970.

[22] F. C. Nix and D. MacNair, «The thermal expansion of pure metals: copper, gold, aluminum, nickel, and iron,» *Physical Review,* vol. 60, p. 597, 1941.

[23] J. C. Wilson, «The thermal expansion of aluminium: Further experiments,» *Proceedings of the Physical Society,* vol. 54, p. 487, 1942.

[24] A. J. Leadbetter, «Anharmonic effects in the thermodynamic properties of solids II. Analysis of data for lead and aluminium,» *Journal of Physics C: Solid State Physics,* vol. 2, p. 1489, 1968.

[25] J. Awbery, and J. E. Griffiths, «The latent heat of fusion of some metals,» *Proceedings of the Physical Society of London,* vol. 38, n. 1, pp. 378-398, 1926.

[26] D. M. Speros and R. L. Woodhouse, «Realization of quantitative differential thermal analysis. I Heat and rates of solid-liquid transition,» *The Journal of Physical Chemistry,* vol. 67, p. 2164, 1963.

[27] F. Uffelmann, «LXI. The expansion of metals at high temperatures,» *The London, Edinburgh, and Dublin Philosophical Magazine and Journal of Science,* vol. 7, pp. 633-659, 1930.

[28] E. R. Jette and F. Foote, «Precision determination of lattice constants,» *The Journal of Chemical Physics,* vol. 3, p. 605, 1935.

[29] J. C. Wilson, «The thermal expansion of aluminium from 0 to 650 C,» *Proceedings of the Physical Society,* vol. 53, p. 235, 1941.

[30] J. W. Richards, «the over-all linear expansion of three face-centered cubic metals (al, cu, pb) from 190 degrees cent to near their melting points,» *Lokale Bestamsangaben,* vol. 82, p. 326, 1942.

[31] «A General-Purpose Debye-Scherrer Camera and its Application to Work at Low Temperatures,» *Journal of Scientific Instruments,* vol. 24, p. 89, 1947.

[32] E. C. Ellwood and J. M. Silcock, «The Lattice Spacings of the Solid Solution of Copper in Aluminium,» *J. Inst. Met,* p. 457, 1948.

[33] A. Kochanovska, «Investigation of thermal dilatation of cubic metals,» *Physica,* n. 1, p. 191, 1949.

[34] W. H.-R. a. T. H. Boultbee, «V. The coefficients of expansion of some solid solutions in aluminium,» *Philosophical Magazine,* n. series 7, 40:300, p. 71, 1949.

[35] Thermal expansion of aluminum and some aluminum alloys, «P. Hidnert and H. S. Krider,» *Journal of Research of the National Bureau of Standards,* vol. 48, n. 3, p. 209, 1952.

[36] A. Smakula and J. Kalnajs, «Precision Determination of Lattice Constants with a Geiger-Counter X-Ray Diffractometer,» *Physical Review,* vol. 99, n. 6, p. 1737, 1955.

[37] B. F. Figgins, G. O. Jones and D. P. Riley, «LXXVII. The thermal expansion of aluminium at low temperatures as measured by an X-ray diffraction method,» *Philosophical Magazine,* vol. 1, n. 8, p. 747, 1956.

[38] D. Gibbons, «Thermal expansion of some crystals with the diamond structure,» *Physical review,* vol. 112, n. 1, p. 136, 1958.

[39] H. M. Otte, «Lattice Parameter Determinations with an X-Ray Spectrogoniometer by the Debye-Scherrer Method and the Effect of Specimen Condition,» *Journal of Applied Physics,* vol. 32, n. 8, p. 1536, 1961.

[40] A. S. Cooper, «Precise lattice constants of germanium, aluminum, gallium arsenide, uranium, sulphur, quartz and sapphire,» *Acta Crystallographica,* vol. 15, n. 6, p. 578, 1962.

[41] H. M. Otte, W. g. Montague and D. O. Welch, «X-Ray Diffractometer Determination of the Thermal Expansion Coefficient of Aluminum near Room Temperature,» *Journal of Applied Physics,* vol. 34.10, p. 3149, 1963.

[42] B. W. Delf, «The practical determination of lattice parameters using the centroid method,» *British Journal of Applied Physics,* vol. 14, n. 6, p. 345, 1963.

[43] R. M. Nicklow and R. A. Young, «Thermal Expansion of AgCl,» *Physical Review,* vol. 129, n. 5, p. 1936, 1963.

[44] A. J. Cornish and J. Burke, «A high temperature attachment for an X-ray diffractometer for precision lattice parameter measurements,» *Journal of Scientific Instruments,* vol. 42, p. 212, 1965.

[45] P. D. Pathak and N. G. Vasavada, «Thermal expansion and the law of corresponding states,» *Journal of Physics C: Solid State Physics,* vol. 3, n. 1, p. 44, 1970.

[46] J. G. Collins, G. K. White, «The thermal expansion of aluminum below 35 K,» *Journal of Low Temperature Physics,* vol. 10, n. 1, p. 69, 1973.

[47] F. R. Kroeger and C. A. Swenson, «Absolute linear thermal-expansion measurements on copper and aluminum from 5 to 320 K,» *Journal of Applied Physics,* vol. 48, n. 3, p. 853, 1977.

[48] J. Bandyopadhyay and K. P. Gupta, «Low-Temperature Lattice Parameters of Al and Al-Zn Alloys and Gruneisen Parameter of Al,» *Cryogenics,* p. 54, 1978.

[49] G. N. Kamm and G. A. Alers, «Low-Temperature Elastic Moduli of Aluminum,» *Journal of Applied Physics,* vol. 35, n. 2, p. 327, 1964.

[50] D. Gerlich and E. S. Fisher, «The high temperature elastic moduli of aluminum,» *Journal of Physics and Chemistry of Solids,* vol. 30, p. 1197, 1969.

[51] J. F. Thomas, «Third-order elastic constants of aluminum,» *Physical Review,* vol. 175, n. 3, p. 955, 1968.

[52] P. S. Ho and A. L. Ruoff, «Pressure dependence of the elastic constants for aluminum from 77 to 300 K,» *Journal of Applied Physics,* vol. 40, n. 8, p. 3151, 1969.

[53] R. Feder and A. S. Nowick, «Use of thermal expansion measurements to detect lattice vacancies near the melting point of pure lead and aluminum,» *Physical Review,* vol. 109, n. 6, p. 1959, 1958.

[54] S. Nenno and J. W. Kauffman, «Detection and Determination of Equilibrium Vacancy Concentrations in Aluminum,» *Journal of the Physical Society of Japan,* vol. 15, n. 2, p. 220, 1960.

[55] R. O. Simmons and R. W. Balluffi, «Measurements of equilibrium vacancy concentrations in aluminum,» *Physical Review,* vol. 117, n. 1, p. 52, 1960.

[56] D. King, A. J. Cornish and J. Burke, «Technique for Measuring Vacancy Concentrations in Metals at the Melting Point,» *Journal of Applied Physics,* vol. 37, n. 13, p. 4714, 1966.

[57] B. von Guerard, H. Peisl and R. Zitzmann, «Equilibrium vacancy concentration measurements on aluminum,» *Applied physics,* vol. 3, p. 37, 1974.

[58] K. Wang and R. R. Reeber, «The perfect crystal, thermal vacancies and the thermal expansion coefficient of aluminium,» *Philosophical Magazine A,* vol. 80, n. 7, p. 1629, 2000.

[59] B. Grabowski, L. Ismer, T. Hickel and J. Neugebauer, «Ab initio up to the melting point: Anharmonicity and vacancies in aluminum,» *Physical Review B ,* vol. 79, n. 13, pp. 1-6, 2009.

[60] T. H. Hehenkamp, «Absolute vacancy concentrations in noble metals and some of their alloys,» *Journal of Physics and Chemistry of Solids,* vol. 55, n. 10, p. 907, 1994.

[61] A. Glensk, B. Grabowski, T. Hickel, and J. Neugebauer, « Breakdown of the arrhenius law in describing vacancy formation energies: The importance of local anharmonicity revealed by Ab initio thermodynamics.,» *Phys. Rev. X,* vol. 4, pp. 1-9, 2014.

[62] O. P. Gupta, «Lattice vibrations and thermophysical properties of aluminium,» *Il Nuovo Cimento D,* vol. 2, n. 1, p. 87, 1983.

[63] D. C. Wallace, «Lattice Dynamical Calculation of Some Thermodynamic Properties for Aluminum,» *Physical Review B,* vol. 1, n. 10, p. 3963, 1970.

[64] T. Soma, T. Itoh and H. Kagaya, «Pressure Effect on Phonon Frequencies and Elastic Stiffness Constants of Al,» *physica status solidi (b),* vol. 125, p. 107, 1984.

[65] T. Soma, S. Nehashi and H. Kagaya, «Specific Heat and Thermal Expansion Coefficient of Al,» *physica status solidi (b),* vol. 130, p. 11, 1985.

[66] M Zoli and V. Bortolani, «Thermodynamic properties of FCC metals: Cu and Al,» *Journal of Physics: Condensed Matter,* vol. 2, p. 525, 1990.

[67] X. J. Kong, C. T. Chan, K. M. Ho and Y. Y. Ye, «Cohesive properties of crystalline solids by the generalized gradient approximation,» *Physical Review B,* vol. 42, n. 15, p. 9357, 1990.

[68] G. K.Straub, J. B. Aidun, J. M. Wills, C. R. Sanchez-Castro and D. C. Wallace, «Ab initio calculation of melting and thermodynamic properties of crystal and liquid aluminum.,» *Physical review. B, Condensed matter,* vol. 50, n. 8, p. 5055, 1994.

[69] G. de Wijs, G. Kresse and M. Gillan, «First-order phase transitions by first-principles free-energy calculations: The melting of Al,» *Physical Review B,* vol. 57, n. 14, p. 8223, 1998.

[70] B. J. Jesson and P. A. Madden, «Ab initio determination of the melting point of aluminum by thermodynamic integration,» *The Journal of Chemical Physics,* vol. 113, n. 14, p. 5924, 2000.

[71] M. Forsblom, N. Sandberg and G. Grimvall, «Anharmonic effects in the heat capacity of Al,» *Physical Review B,* vol. 69, n. 16, p. 165106, 2004.

[72] M. Forsblom and G. Grimvall, «Heat capacity of liquid Al: Molecular dynamics simulations,» *Physical Review B,* vol. 72, n. 13, p. 132204, 2005.

[73] S. Hayat, M. Choudhry and S. Ahmad, «Effect of twin-boundaries on melting of aluminum,» *Journal of Materials Science,* vol. 43, n. 14, p. 4915, 2008.

[74] M. Jacobs and R. Schmid-Fetzer, «Thermodynamic properties and equation of state of fcc aluminum and bcc iron, derived from a lattice vibrational method,» *Physics and Chemistry of Minerals,* vol. 37, n. 10, p. 721, 2010.

[75] N. K. Bhatt, B. y. Thakore, P. R. Vyas and a. R. Jani, «High-Temperature Vibrational Properties and Melting Curve of Aluminum,» *International Journal of Thermophysics,* vol. 31, n. 11, p. 2159, 2010.

[76] A. Hänström and P. Lazor, «High pressure melting and equation of state of aluminium,» *Journal of alloys and compounds,* vol. 305, p. 209, 2000.

[77] L. Vočadlo and A. Dario, «Ab initio melting curve of the fcc phase of aluminum,» *Physical Review B,* vol. 65, n. 21, p. 214105, 2002.

[78] A. Dario, «First-principles simulations of direct coexistence of solid and liquid aluminum,» *Physical Review B,* vol. 68, n. 6, p. 064423, 2003.

[79] J. Bouchet, F. Bottin, G. Jomard and G. Zérah, «Melting curve of aluminum up to 300 GPa obtained through ab initio molecular dynamics simulations,» *Physical Review B,* vol. 80, n. 9, p. 094102, 2009.

[80] R. Boehler and M. Ross, «Melting curve of aluminum in a diamond cell to 0.8 Mbar: implications for iron,» *Earth and Planetary Science Letters,* vol. 153, p. 223, 1997.

[81] X-G Lu, M. Selleby and B. Sundman, «Assessments of molar volume and thermal expansion for selected bcc, fcc and hcp metallic elements,» *Calphad,* vol. 29, n. 1, p. 68, 2005.

[82] B. Hallstedt, «Molar volumes of Al, Li, Mg and Si,» *Calphad,* vol. 31, n. 2, p. 292, 2007.

[83] P. Desai, «Thermodynamic properties of aluminum,» *International journal of thermophysics,* vol. 8, n. 5, pp. 621-638, 1987.

[84] A. Duff, M. Finnis, P. Maugis, B. Thijsse and M. Sluiter, «MEAMfit: A reference-free modified embedded atom method (RF-MEAM) energy and force-fitting code,» *Computer Physics Communications,* vol. 169, pp. 439-445, 2015.

[85] A. I. Duff, T. Davey, D. Korbmacher, A. Glensk, B. Grabowski, J. Neugebauer, and M. W. Finnis, «Improved method of calculating ab initio high-temperature thermodynamic properties with application to ZrC,» *Physical Review B,* vol. 91, n. 21, p. 214311, 2015.

[86] L. Zhu, B. Grabowski, and J. Neugebauer, «Improved method to effciently compute melting properties fully from ab initio with application to Cu,» *Phys. Rev. B,* vol. 96, n. 22, p. 224202, 2017.

[87] J. R. Morris, C.Z. Wang, K. M. Ho and C. T. Chan, «Melting line of aluminum from simulations of coexisting phases,» *Physical Review B,* vol. 49, n. 5, pp. 3109-3115, 1994.

[88] Q.S. Mei and K. Lu , «Melting and superheating of crystalline solids,» *Progress in Materials Science ,* vol. 52, p. 1175–1262, 2007.

[89] B. J. Siwick, J. R. Dwyer, R. E. Jordan and R.J. Dwayne Miller , «Femtosecond electron diffraction studies of strongly driven,» *Chemical Physics ,* vol. 299, p. 285–305, 2004.

[90] Y. S. Hwang and V. I. Levitas, «Superheating and melting within aluminum core–oxide shell nanoparticles for a broad range of heating rates: multiphysics phase field modeling,» *Phys.Chem.Chem.Phys.,* vol. 18, p. 28835 , 2016.

[91] Y. Kraftmakher, Lecture Notes on Equilibrium Point Defects and Thermophysical Properties of Metals, World Scientific, 2000.

[92] D. C. Hopkins, PhD thesis, Univercity of Illinois, 1962.

[93] C. G. Maier and C. T. Anderson, «The disposition of work energy applied to crystals,» *The Journal of Chemical Physics,* vol. 2, pp. 513-527, 1934.

[94] D. B Downie and J. F. Martin, «An adiabatic calorimeter for heat-capacity measurements between 6 and 300 K. The molar heat capacity of aluminium,» *The Journal of Chemical Thermodynamics,* vol. 12, pp. 779-786, 1982.

[95] W, Kramer and J. Nölting, «Anomale spezifische Wärmen und fehlordnung der Metalle indium, Zinn, Blei, Zink, Antimon und Aluminium,» *Acta Metallurgica,* vol. 20, n. 12, pp. 1353-1359, 1972.

[96] R. Stedman and G. Nilsson, «Dispersion relations for phonons in aluminum at 80 and 300 K,» *Physical Review,* vol. 145, n. 2, p. 492, 1966.

[97] R. Stedman, L. Almqvist and G. Nilsson, «Phonon-frequency distributions and heat capacities of aluminum and lead,» *Physical Review,* vol. 162, n. 3, p. 549, 1967.

[98] M. Kresch, M. Lucas, O. Delaire, J. Lin and B. fultz, «Phonons in aluminum at high temperatures studied by inelastic neutron scattering,» *Physical Review B,* vol. 77, n. 2, p. 024301, 2008.

[99] W. T. Berg, «Heat capacity of Aluminum between 2.7 and 20 K,» *Physical Review,* vol. 167, n. 3, pp. 583-586, 1968.

[100] A. Gupta, B. Kavakbasi, B. Dutta, B. Grabowski, M. Peterlechner, T. Hickel, S. V. Divinski, G. Wilde, and J. Neugebauer, «Low-temperature features in the heat capacity of unary metals and intermetallics for the example of bulk aluminum and Al3Sc,» *Physical review B,* vol. 95, p. 094307, 2017.

[101] «A General-Purpose Debye-Scherrer Camera and its Application to Work at Low Temperatures,» *Journal of Scientific Instruments,* vol. 24, p. 89, 1947.

[102] W. H.-R. a. T. H. Boultbee, «V. The coefficients of expansion of some solid solutions in aluminium,» *Philosophical Magazine,* n. series 7, 40:300, p. 71, 1949.

[103] Thermal expansion of aluminum and some aluminum alloys, «P. Hidnert and H. S. Krider,» *Journal of Research of the National Bureau of Standards,* vol. 48, n. 3, p. 209, 1952.

[104] H. M. Otte, W. g. Montague and D. O. Welch, «X-Ray Diffractometer Determination of the Thermal Expansion Coefficient of Aluminum near Room Temperature,» *Journal of Applied Physics,* vol. 34.10, p. 3149, 1963.

[105] D. C. Wallace, «Lattice Dynamical Calculation of Some Thermodynamic Properties for Aluminum,» *Physical Review B,* vol. 1, n. 10, p. 3963, 1970.

[106] M. Zoli and V. Bortolani, «Thermodynamic properties of FCC metals: Cu and Al,» *Journal of Physics: Condensed Matter,* vol. 2, p. 525, 1990.

View publication stats